

Published in final edited form as:

*Magn Reson Med.* 2011 April ; 65(4): 956–963. doi:10.1002/mrm.22792.

## Time Resolved Contrast Enhanced Intracranial MRA Using a Single Dose Delivered as Sequential Injections and Highly Constrained Projection Reconstruction (HYPR CE)

Yijing Wu<sup>1,\*</sup>, Kevin Johnson<sup>1</sup>, Steven R. Kecsckemeti<sup>1</sup>, Kang Wang<sup>1</sup>, Oliver Wieben<sup>1,2</sup>, Beverly L. Aagaard-Kienitz<sup>2</sup>, Howard Rowley<sup>2</sup>, Frank R. Korosec<sup>2</sup>, Charles Mistretta<sup>1,2</sup>, and Patrick Turski<sup>2</sup>

<sup>1</sup>Department of Medical Physics, University of Wisconsin, Madison, Wisconsin, USA.

<sup>2</sup>Department of Radiology, University of Wisconsin, Madison, Wisconsin, USA.

### Abstract

Time-resolved contrast-enhanced magnetic resonance angiography of the brain is challenging due to the need for rapid imaging and high spatial resolution. Moreover, the significant dispersion of the intravenous contrast bolus as it passes through the heart and lungs increases the overlap between arterial and venous structures, regardless of the acquisition speed and reconstruction window. An innovative technique is presented that divides a single dose contrast into two injections. Initially a small volume of contrast material (2–3 mL) is used to acquiring time-resolved weighting images with a high frame rate (2 frames/s) during the first pass of the contrast agent. The remaining contrast material is used to obtain a high resolution whole brain contrast-enhanced (CE) magnetic resonance angiography ( $0.57 \times 0.57 \times 1 \text{ mm}^3$ ) that is used as the spatial constraint for Local Highly Constrained Projection Reconstruction (HYPR LR) reconstruction. After HYPR reconstruction, the final dynamic images (HYPR CE) have both high temporal and spatial resolution. Furthermore, studies of contrast kinetics demonstrate that the shorter bolus length from the reduced contrast volume used for the first injection significantly improves the arterial and venous separation.

### Keywords

time-resolved MRA; contrast enhanced; MRA; constrained reconstruction

## INTRODUCTION

Angiographic techniques such as digital subtraction angiography have demonstrated the value of time resolved imaging for the diagnosis of intracranial vascular disease (1). However, X-ray digital subtraction angiography requires arterial injection, employs ionizing radiation and uses potentially nephrotoxic contrast material. High resolution time-resolved contrast-enhanced magnetic resonance angiography (TR CE MRA) is of very low risk and is advantageous for the detection of differential vascular filling due to high-flow lesions such as brain arteriovenous malformations and dural fistulas (1,2). Several strategies to increase spatial and temporal resolution in TR CE MRA have been introduced (3–9). However, the inherent trade-off between the temporal resolution, spatial resolution and SNR limits their

clinical applications. Furthermore, the length of the contrast bolus, after circulation through lung and heart increases the difficulty in separating fast and slow flow vascular structures.

The Hybrid HYPR (10–13) methods, split the tasks of providing spatial resolution/SNR and temporal resolution between two scans and uses HYPR LR reconstruction to obtain a time series of images with improved image quality (14). Decoupling of the temporal resolution and SNR also allows for a reduction in the first pass contrast dose to as low as 2 mL without significant degradation the final HYPR LR dynamic series image quality (15). Although HYPR LR reconstruction can be performed using a post contrast phase-contrast using vastly undersampled isotropic projection reconstruction (PC VIPR) exam or pre contrast time-of-flight images as the spatial constraint, these methods are susceptible signal loss due to dephasing from complex flow or saturation of slow flow. In such regions, the final HYPR LR images will lose vascular signal and SNR (13,16).

For Hybrid HYPR, a desirable spatial constraint would minimize signal loss and have high resolution of both arteries and veins. This can be achieved to some degree by using a contrast enhanced whole brain acquisition. However, it is not clinically desirable to significantly increase the contrast dose due to the NSF concern and the additional cost. In this report we demonstrate the value of splitting a single contrast dose into two injections. The first small injection is used for the low resolution TR CE MRA weighting images. The remaining contrast is injected to obtain a high resolution contrast enhanced MRA acquisition that is used as the spatial constraint for HYPR reconstruction. The final HYPR CE images are a set of time resolved angiograms with temporal resolution equivalent to the weighting images acquired during the first injection and the spatial resolution and SNR comparable to the high resolution CE MRA acquired during the second injection. We show that HYPR CE not only is able to provide improved vascular depiction, but also has excellent arterial-venous separation due to the short contrast bolus.

## MATERIALS AND METHODS

All exams were performed on a standard 3T MR system (GE Healthcare) with an eight-channel head coil. Contrast agent injections were administered using an MR-compatible, computer-controlled power injector (Medrad, Indianola, PA) through an intravenous catheter placed in the antecubital fossa. In all cases, subjects were scanned after providing written informed consent according to an approved protocol and guidelines outlined by our institutional review board.

### Volunteer Studies

HYPR CE exams were obtained in seven normal volunteers, two patients with intracranial aneurysms and one patient with a brain arteriovenous malformations and one patient with a dural arterio-venous fistula. For each study, a single dose (0.1 mmol/kg) of gadolinium-based contrast agent was split into two injections. The first small injection (2–3 mL) was administered at 3 mL/s followed by a 25 mL saline flush, starting simultaneously with a time-resolved multiecho VIPR (ME VIPR) acquisition (17,18). The second injection (the remainder of the single dose of the contrast agent) was administered at 0.5 mL/s followed by a 20 mL saline flush (19). A high resolution CE MRA was acquired with elliptical centric view ordering and fluoro-trigger technique. The imaging parameters for ME VIPR were: FOV =  $22 \times 22 \times 22$  cm<sup>3</sup> TR/TE = 3.1/0.4 ms, BW = 125 kHz, read out points were 128 per projection, resulting in the acquired voxel size:  $1.7 \times 1.7 \times 1.7$  mm<sup>3</sup>, frame update time was 0.5 s. The imaging parameters for the high resolution CE MRA were: FOV =  $22 \times 22 \times 22$  cm<sup>3</sup>, TR/TE = 5.4/1.9 ms, BW = 62.4 kHz, acquisition matrix =  $384 \times 384 \times 160$ , slice thickness = 1 mm, acquired voxel size was:  $0.57 \times 0.57 \times 1$  mm<sup>3</sup>. Factor of  $2 \times 2$  parallel imaging was applied to reduce the scan time to within 90 sec.

To assess the impact of the two contrast volumes (a standard single dose [0.1 mmol/kg] and a small dose [2-mL]) on arterial-venous separation, as well as image quality a phase-contrast HYPRFLOW (PC HYPRFlow) (12,16) exam was obtained for the seven volunteer studies and one patient with a partially treated mid basilar artery aneurysm. The PC HYPRFlow scan was acquired either before or after the HYPR CE exam with 20 minutes in between to minimize the effects of residual contrast. The imaging protocol for the PC HYPRFlow exam was as follows: a TR ME VIPR acquisition was started simultaneously with a single dose injection (0.1 mmol/kg) administered at 3 mL/s followed by 20 mL saline flush. A post contrast phase-contrast VIPR (PC VIPR) acquisition was started immediately after the dynamic scan and was used as the spatial constraint. The imaging parameters for TR ME VIPR were same as those in the HYPR CE study. The imaging parameters for the PC VIPR acquisition were: FOV =  $22 \times 22 \times 22$  cm<sup>3</sup>, TR/TE = 12.5/4.8 ms, VENC = 80 cm/s, BW = 83.4 kHz; Readout matrix were 320 points per projection, acquired voxel size was  $0.69 \times 0.69 \times 0.69$  mm<sup>3</sup>. Seven thousand projections were acquired within 5 minutes.

### Reconstruction Scheme

The reconstruction scheme for HYPR CE is same as other hybrid HYPR techniques (16,20) and can be formulated as the temporal weighting image ( $I_w^t$ ) multiplied by the composite ( $I_C$ ), which is performed using HYPR LR algorithm (14) as following:

$$I_H(t) = I_w^t \cdot I_C = \frac{I_t \otimes K}{I_C^t \otimes K} \cdot I_C$$

Where  $I_t$  is a conventionally reconstructed time frame image from the ME VIPR scan,  $I_C$  is the composite image, in our case the high resolution CE image,  $I_C^t$  is the reprojected composite image along the same trajectory as the current time frame image  $I_t$ , and  $K$  is the convolution kernel. The equivalent kernel size is about  $10 \times 10 \times 10$  pixels. To compensate the signal variations due to the high undersampling, a tornado filter (17) was used with 0.5 s at the central  $k$ -space and 0.75 s at the cutoff frequency of the local kernel being applied. Such temporal weighting images feature of high temporal resolution and high SNR but low spatial resolution due to low pass filtering and low acquired resolution. The high resolution CE composite image provides the vascular map with high spatial resolution and high SNR. When the composite is multiplied by the weighting images, the result is a time series with the spatial resolution of the CE MRA composite ( $0.57 \times 0.57 \times 1.0$  mm<sup>3</sup>) and temporal resolution of 0.75 s.

### Image Assessment

To compare the arterial-venous separation for a single dose/single injection (using a PC VIPR constraint) and a dual injection (using a CE MRA constraint), regions-of-interest (ROIs) were drawn at the same locations in the images generated by the two techniques. An arterial ROI was drawn on the basilar artery and a venous ROI was drawn on the superior sagittal sinus. Contrast kinetic curves (signal versus time curve) from the arterial and venous ROIs were generated for each volunteer. Full width at half maximum (FWHM) was measured based on each contrast kinetic curve (21). A shorter FWHM indicates a tighter bolus and better temporal separation of arterial and venous signals. The ratio between arterial and venous signals at the peak arterial frame (A/V ratio) and ratio between venous and arterial signals at the peak venous frame (V/A ratio) were calculated. The higher A/V and V/A ratios mean better arterial venous separation. In addition, the overlap of arterial and venous signal (overlap integral) was also calculated as (22):

$$O = \sum_{n=1}^N \min \left( \frac{A[n]}{\sum_{m=1}^N A[m]}, \frac{V[n]}{\sum_{m=1}^N V[m]} \right),$$

where  $A[n]$  and  $V[n]$  are the arterial and venous signals at time frame  $n$ ,  $N$  is the total number of time frames. This integral calculates the area of the overlapped region between arterial and venous contrast kinetic curves. A smaller overlap integral implies better arterial and venous separation. Two-tailed paired  $t$ -tests were conducted to determine whether the difference between two techniques (PC HYPRFLOW with single injection and HYPR CE with dual injection) was significant.

## RESULTS

All HYPR CE exams were reconstructed off-line using in-house reconstruction software. The serial images were used to investigate the contrast kinetics. Figure 1 displays four representative time frames from the 60 time frame HYPR CE exam (normal volunteer subject) in the axial, coronal and sagittal planes. The arterial and venous phase images (shown in column 1 and 4) show well delineated arterial and venous structures with excellent arterial/venous separation. The mix phases (as shown in column 2 and 3) show the distal vessels to better advantage.

For the subjects with both HYPR CE and PC HYPRFlow exams (including seven volunteers and one aneurysm patient), both series were reviewed by a radiologist, all exams were considered technically satisfactory for the comparison evaluation. For all seven volunteer exams, HYPR CE and PC HYPRFlow series were both able to represent the contrast dynamics with excellent temporal and spatial resolution. The benefit of using CE MRA as the spatial constraint (HYPR CE) was observed in the aneurysm patient. Figure 2 shows a mid basilar artery aneurysm previously treated using detachable coils. The PC HYPRFlow image (a) does not clearly demonstrate the residual flow within the aneurysm due to susceptibility artifacts from the coils and slow flow within the aneurysm. The HYPR CE image (b) is able to detect the residual flow. Digital subtraction angiography (c) and the high resolution CE MRA (shown in Fig. 3) confirmed the presence of the residual lumen.

The improvement of spatial resolution and SNR of HYPR CE over the VIPR images reconstructed using gridding technique can be observed in Fig. 3 from the same aneurysm patient, where limited MIPs from one time frame of VIPR images (a), HYPR CE images (b) and the high resolution CE MRA image (c) were compared. VIPR images were zero-filled to the same matrix size as the other image sets for better comparison. Line profiles across the aneurysm as shown in Fig. 3c were compared in Fig. 3d. The residual aneurysm lumen matches closely between HYPR CE and the high resolution CE images, whereas low resolution VIPR image shows blurred edge compared to the high resolution CE image.

For the two patients with high flow lesions (arteriovenous malformations, dural arteriovenous fistula), the HYPR CE exams were able to identify the early arterial enhancement and drainage veins. Figure 4 shows a patient with a left transverse sinus dural arterio-venous fistula. The HYPR CE time frames demonstrate the early filling of the left transverse sinus indicating rapid shunting into the dural sinus (arrows).

Qualitative and quantitative evaluations of the effect of the contrast volume on the arterial and venous separation were conducted on the seven volunteers. Figure 5 shows venous phase images at corresponding times from (a) PC HYPRFlow with full single dose injected

during the dynamic acquisition and (b) HYPR CE exams with single dose dual injections. The shorter bolus resulting from the smaller contrast volume of the HYPR CE technique improves the arterial venous separation. Note that arterial signal from the longer contrast bolus is present in the PC HYPRFlow image.

Figure 6 shows the arterial and venous contrast kinetic curves obtained using PC HYPRFlow (a) and HYPR CE (b) techniques from the same volunteer as in Fig. 5. For HYPR CE technique, the significant shorter FWHM from both arterial and venous ROIs and smaller overlap integral, which can be visualized as the area under the overlapped curves, have been observed, which indicate better arterial venous separation.

Figure 7 compares the FWHM (a) and the overlap integral (b) between HYPRFlow with full single dose injection and HYPR CE with single dose dual injections for all seven volunteers. The FWHM and the overlap integral obtained from the HYPR CE technique with smaller contrast volume injected during the dynamic acquisition are significantly smaller than those obtained from the HYPRFlow with full single dose injection technique, which implies better arterial and venous separation.

Table 1 lists the results of the comparison between PC HYPRFlow using the conventional single dose injection and HYPR CE using single dose dual injection. For all the parameters measured in this article (FWHM,  $A/V$ ,  $V/A$  and overlap integral), the two techniques exhibited significant difference ( $P < 0.05$ ).

## DISCUSSION

For time-resolved contrast enhanced MRA, trade-offs between temporal and spatial resolution limit the overall achievement. HYPR methods (16,20), for the first time, decouple the high temporal resolution, which requires fast acquisition, from the high spatial resolution and SNR, which demands longer scan time, thus achieving high temporal resolution, high spatial resolution and high SNR simultaneously. High resolution CE MRA provides the most accurate vascular definition, however it has never been used as the spatial constraint for the TR CE MRA due to the need for extra contrast volume. The SNR property of HYPR reconstruction is able to reduce the contrast dosage of the dynamic acquisition to as little as 1–3 mL without significantly degrading the image quality (15). HYPR CE splits a single contrast volume into two injections, the first small injection (2–3 mL) provides enough contrast for low resolution weighting images and the second injection with the rest of volume ensures excellent SNR for the high resolution CE MRA as the spatial constraint (23). With HYPR reconstruction, a series of time-resolved contrast enhanced MRA with both high temporal and spatial resolution can be obtained. Unlike other HYPR techniques (PC HYPRFlow and HYPR time-of-flight), HYPR CE does not suffer from signal ambiguities due to the different contrast mechanisms. Therefore, it provides accurate filling dynamics and vascular anatomy.

Improving temporal resolution is a goal for TR CE MRA. However, increasing the frame rate alone is not adequate to improve the arterial-venous separation due to the significant dispersion of the contrast bolus resulting from the circulation through the heart and lungs after the venous injection. Our results show that when the contrast bolus length is shortened by the reduction of the contrast volume, combined with highly under-sampled acquisition and constrained reconstruction, the result is improved arterial venous separation. It should be noted that the improvement of a/v separation is based on the dynamic weighting images, specifically, how much contrast volume being admitted during the dynamic acquisition and is independent of the constraining image (HYPR CE or PC HYPRFlow).

A “test bolus” has been used in clinical applications to determine arrival time for the following high resolution CE MRA. However, the dynamic “test bolus” images are not often used for evaluating the vascular hemodynamics due to limited coverage, low spatial resolution and low SNR (7,24). HYPR CE takes full advantage of the high temporal resolution and tight bolus from the “test bolus” weighting images and the high spatial resolution from the high resolution CE MRA as the spatial constraint, resulting in better arterial venous separation with comparable spatial resolution and SNR than those using the regular single dose dynamic scan as the temporal weighting. This is extremely useful for cases in which there is differential filling of vessels due to arterial stenosis or rapid shunting as may be encountered in a brain arteriovenous malformations. Since HYPR CE involves two scans, patient motion is a concern. In the case when the subject moves between two scans, image registration between two scans can be applied by using a fully automated linear image registration tool (FLIRT) before HYPR LR reconstruction. Since motion of head is rigid, FLIRT has been shown to be very robust (11–12).

## CONCLUSIONS

HYPR CE provides time resolved contrast enhanced images with subsecond temporal resolution, submillimeter spatial resolution and high SNR with total scan times of less than 150 seconds.

## Acknowledgments

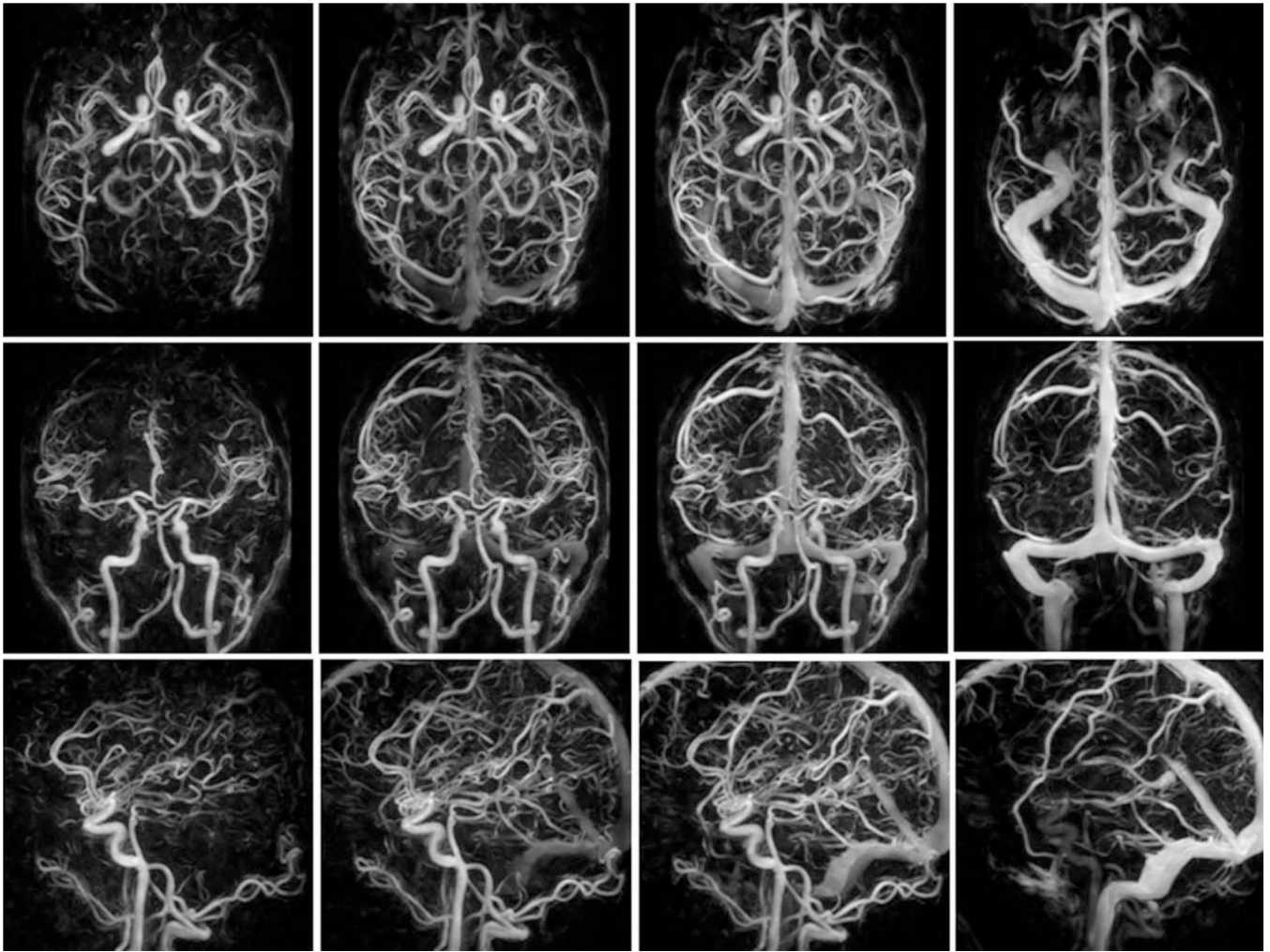
The authors thank Kelli Hellenbrand and Sara Pladziewicz for helping the volunteer scans.

Grant sponsors: NIH: R01NS066982-01; R21EB009441-01; R01EB006882-01.

## REFERENCES

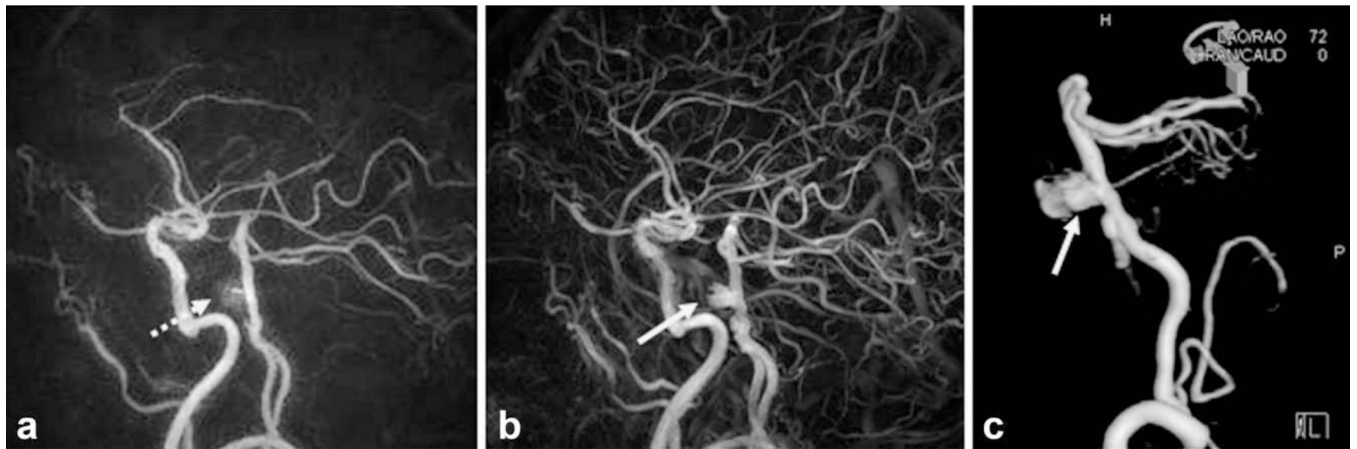
1. Kwan ES, Hall A, Enzmann DR. Quantitative analysis of intracranial circulation using rapid-sequence DSA. *AJR Am J Roentgenol.* 1986; 146:1239–1245. [PubMed: 3518369]
2. Marchal G, Bosmans H, Van Fraeyenhoven L, Wilms G, Van Hecke P, Plets C, Baert AL. Intracranial vascular lesions: optimization and clinical evaluation of three-dimensional time-of-flight MR angiography. *Radiology.* 1990; 175:443–448. [PubMed: 2326471]
3. Cashen TA, Jeong H, Shah MK, Bhatt HM, Shin W, Carr JC, Walker MT, Batjer HH, Carroll TJ. 4D radial contrast-enhanced MR angiography with sliding subtraction. *Magn Reson Med.* 2007; 58:962–972. [PubMed: 17969099]
4. Haider CR, Hu HH, Campeau NG, Huston J III, Riederer SJ. 3D high temporal and spatial resolution contrast-enhanced MR angiography of the whole brain. *Magn Reson Med.* 2008; 60:749–760. [PubMed: 18727101]
5. Nael K, Michaely HJ, Villablanca P, Salamon N, Laub G, Finn JP. Time-resolved contrast enhanced magnetic resonance angiography of the head and neck at 3.0 tesla: initial results. *Invest Radiol.* 2006; 41:116–124. [PubMed: 16428982]
6. Cashen TA, Carr JC, Shin W, Walker MT, Futterer SF, Shaibani A, McCarthy RM, Carroll TJ. Intracranial time-resolved contrast-enhanced MR angiography at 3T. *AJNR Am J Neuroradiol.* 2006; 27:822–829. [PubMed: 16611772]
7. Kramer U, Fenchel M, Laub G, Seeger A, Klumpp B, Bretschneider C, Finn JP, Claussen CD, Miller S. Low-dose, time-resolved, contrast-enhanced 3D MR angiography in the assessment of the abdominal aorta and its major branches at 3 Tesla. *Acad Radiol.* 2010; 17:564–576. [PubMed: 20171907]
8. Jeong HJ, Cashen TA, Hurley MC, Eddleman C, Getch C, Batjer HH, Carroll TJ. Radial sliding-window magnetic resonance angiography (MRA) with highly-constrained projection reconstruction (HYPR). *Magn Reson Med.* 2009; 61:1103–1113. [PubMed: 19230015]

9. Haider CR, Borisch EA, Glockner JF, Mostardi PM, Rossman PJ, Young PM, Riederer SJ. Max CAPR: high-resolution 3D contrast-enhanced MR angiography with acquisition times under 5 seconds. *Magn Reson Med.* 2010; 64:1171–1181. [PubMed: 20715291]
10. Velikina, J.; Johnson, KM.; Wieben, O.; Turski, P.; Grist, TM.; Mistretta, C. ISMRM workshop on Non-Cartesian MRI. Sedona, AZ: 2007. First pass HYPR flow: time-resolved CE-MRA with 322-fold under-sampling and a phase contrast HYPR composite providing 4-fold SNR restoration per time frame; p. 1
11. Wu, Y.; Johnson, KM.; Velikina, J.; Turski, P.; Mistretta, C. Clinical experience of HYPR FLOW. Proceedings of the 16th Annual Meeting of the ISMRM; Toronto, Ontario. 2008. p. 110
12. Wu Y, Chang W, Johnson KM, Velikina J, Rowley H, Mistretta C, Turski P. Fast whole-brain 4D contrast-enhanced MR angiography with velocity encoding using undersampled radial acquisition and highly constrained projection reconstruction: image-quality assessment in volunteer subjects. *AJNR Am J Neuroradiol.* 2010
13. Wu, Y.; Kecskemeti, S.; Turski, PA.; Mistretta, CA. HYBRID HYPR MRA. Proceedings of the 17th Annual Meeting of ISMRM; Honolulu. 2009. p. P3257
14. Johnson KM, Velikina J, Wu Y, Kecskemeti S, Wieben O, Mistretta CA. Improved waveform fidelity using local HYPR reconstruction (HYPR LR). *Magn Reson Med.* 2008; 59:456–462. [PubMed: 18306397]
15. Wu, YKS.; Johnson, KM.; Turski, PA.; Mistretta, CA. Low dose hybrid HYPR MRA. Proceedings of the 18th Annual Meeting of ISMRM; Stockholm. 2010. p. P3765
16. Velikina JV, Johnson KM, Wu Y, Samsonov AA, Turski P, Mistretta CA. PC HYPR flow: a technique for rapid imaging of contrast dynamics. *J Magn Reson Imaging.* 31:447–456. [PubMed: 20099362]
17. Barger AV, Block WF, Toropov Y, Grist TM, Mistretta CA. Time-resolved contrast-enhanced imaging with isotropic resolution and broad coverage using an undersampled 3D projection trajectory. *Magn Reson Med.* 2002; 48:297–305. [PubMed: 12210938]
18. Lu A, Brodsky E, Grist TM, Block WF. Rapid fat-suppressed isotropic steady-state free precession imaging using true 3D multiple-half-echo projection reconstruction. *Magn Reson Med.* 2005; 53:692–699. [PubMed: 15723411]
19. Carroll TJ, Korosec FR, Swan JS, Hany TF, Grist TM, Mistretta CA. The effect of injection rate on time-resolved contrast-enhanced peripheral MRA. *J Magn Reson Imaging.* 2001; 14:401–410. [PubMed: 11599064]
20. Wu, YJK.; Velikina, J.; Turski, P.; Mistretta, C. Hybrid HYPR MRA. Proceedings of the 17th Annual Meeting of the ISMRM; Honolulu, Hawaii. 2009. p. 3257
21. Raoult H, Ferre JC, Morandi X, Carsin-Nicol B, Carsin M, Cuggia M, Law M, Gauvrit JY. Quality-evaluation scheme for cerebral time-resolved 3D contrast-enhanced MR angiography techniques. *AJNR Am J Neuroradiol.* 2010; 31:1480–1487. [PubMed: 20448014]
22. Cashen TA, Jeong H, Shah MK, Bhatt HM, Shin W, Carr JC, Walker MT, Batjer HH, Carroll TJ. 4D radial contrast-enhanced MR angiography with sliding subtraction. *Magn Reson Med.* 2007; 58:962–972. [PubMed: 17969099]
23. Beranek-Chiu J, Froehlich JM, Wentz KU, Doert AN, Zollikofer CL, Eckhardt BP. Improved vessel delineation in keyhole time-resolved contrast-enhanced MR angiography using a gadolinium doped flush. *J Magn Reson Imaging.* 2009; 29:1147–1153. [PubMed: 19388120]
24. Carroll, TJ. 2nd Madison-Freiburg Workshop on Accelerated Medical Imaging. Madison, WI: 2010. Radial imaging for neurovascular applications. Invited talk

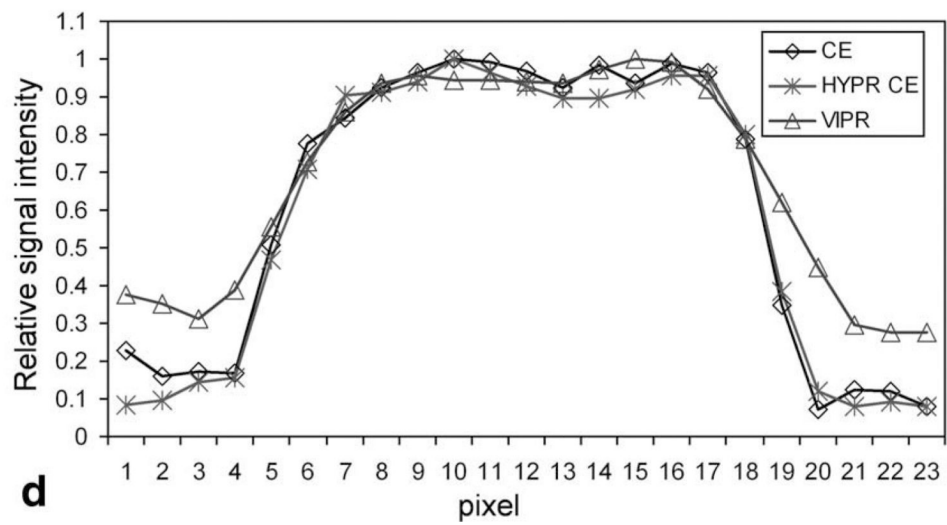
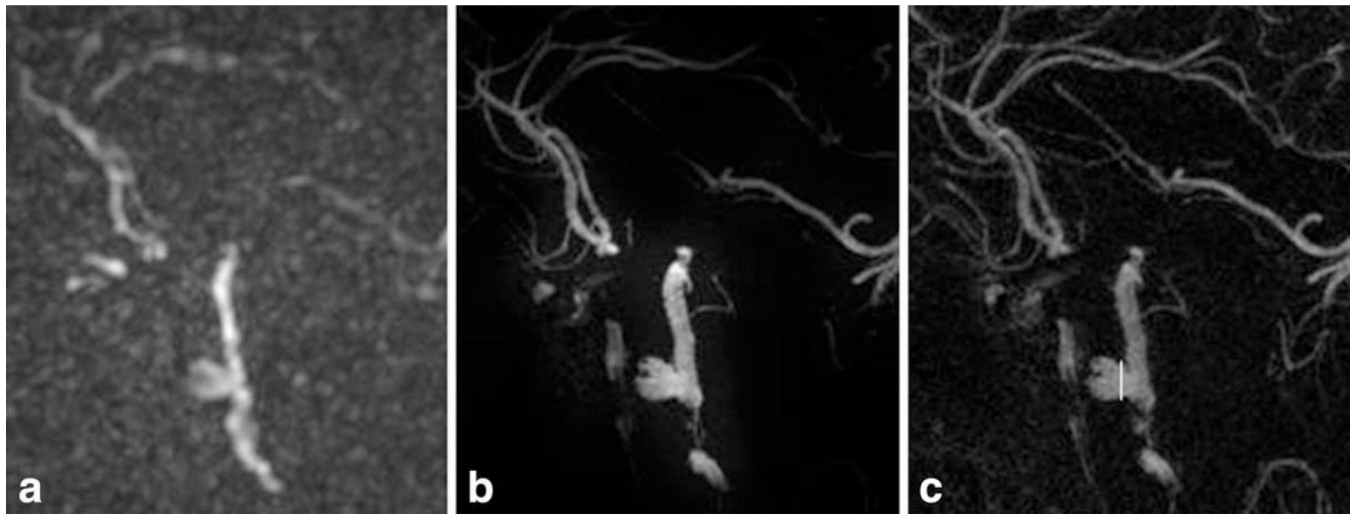


**FIG. 1.** Four time frames from a 60 frame HYPR CE exam are displayed in the axial (top row), coronal (middle row) and sagittal (bottom row) planes. Highly accelerated (undersampled) 3D radial scans are obtained every 0.75 seconds during the first pass of a 2 mL contrast bolus. This is followed by a higher resolution CE MRA of the brain obtained during a longer injection of contrast material. The serial images are reconstructed with HYPR LR using the CE MRA as the constraint. This approach generates time resolved images with the temporal resolution of the undersampled 3D radial acquisition (0.75 s) and the spatial resolution of the CE MRA ( $0.57 \times 0.57 \times 1 \text{ mm}^3$ ).

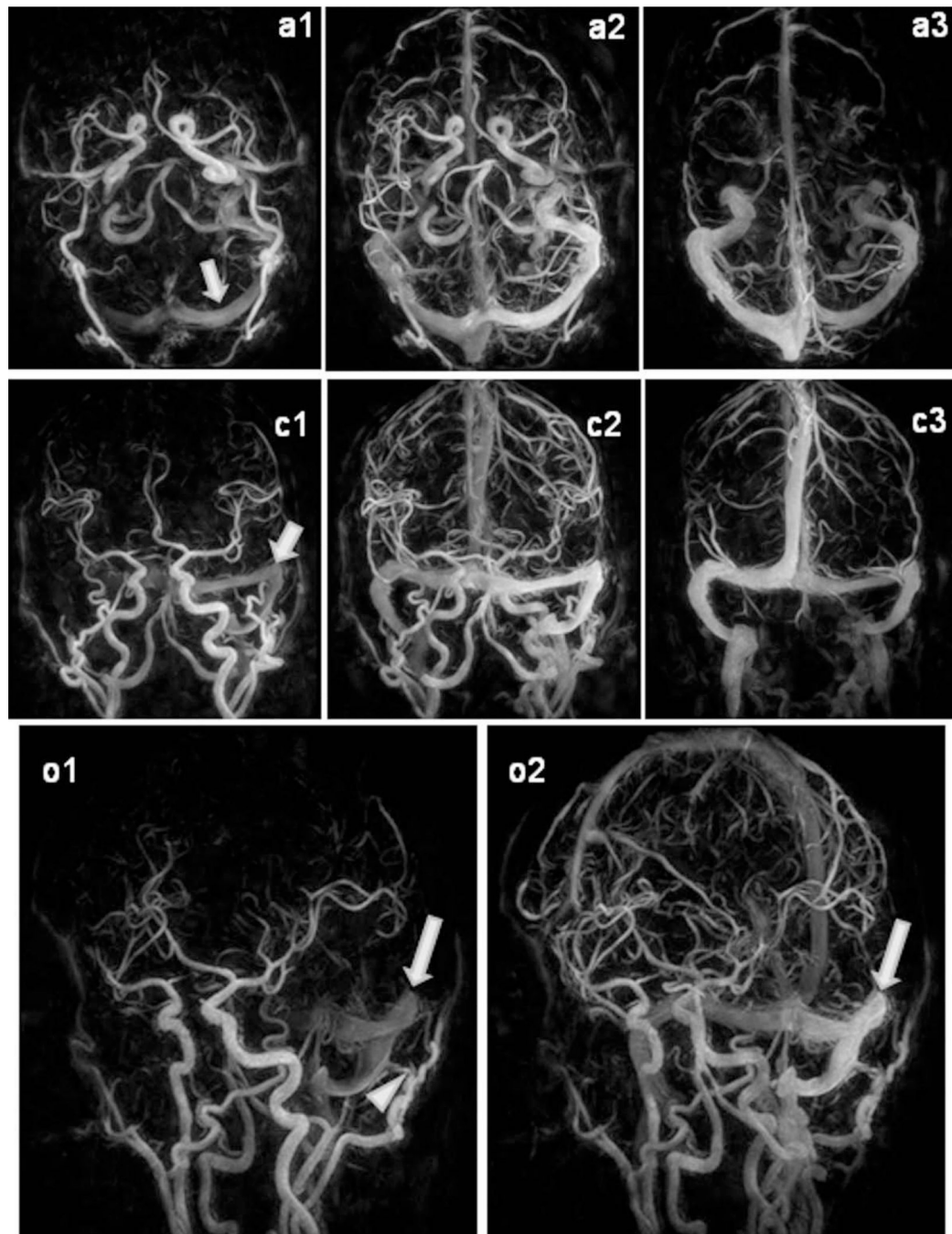




**FIG. 2.** Comparison of HYPR LR reconstruction using (a) the PC VIPR exam as the constraint and (b) using the CE MRA as the constraint with digital subtraction angiography (c) as the gold standard. The patient's mid basilar artery aneurysm was previously treated with detachable coils. The residual aneurysm lumen (arrow) is better appreciated when the CE MRA is used as the constraint.

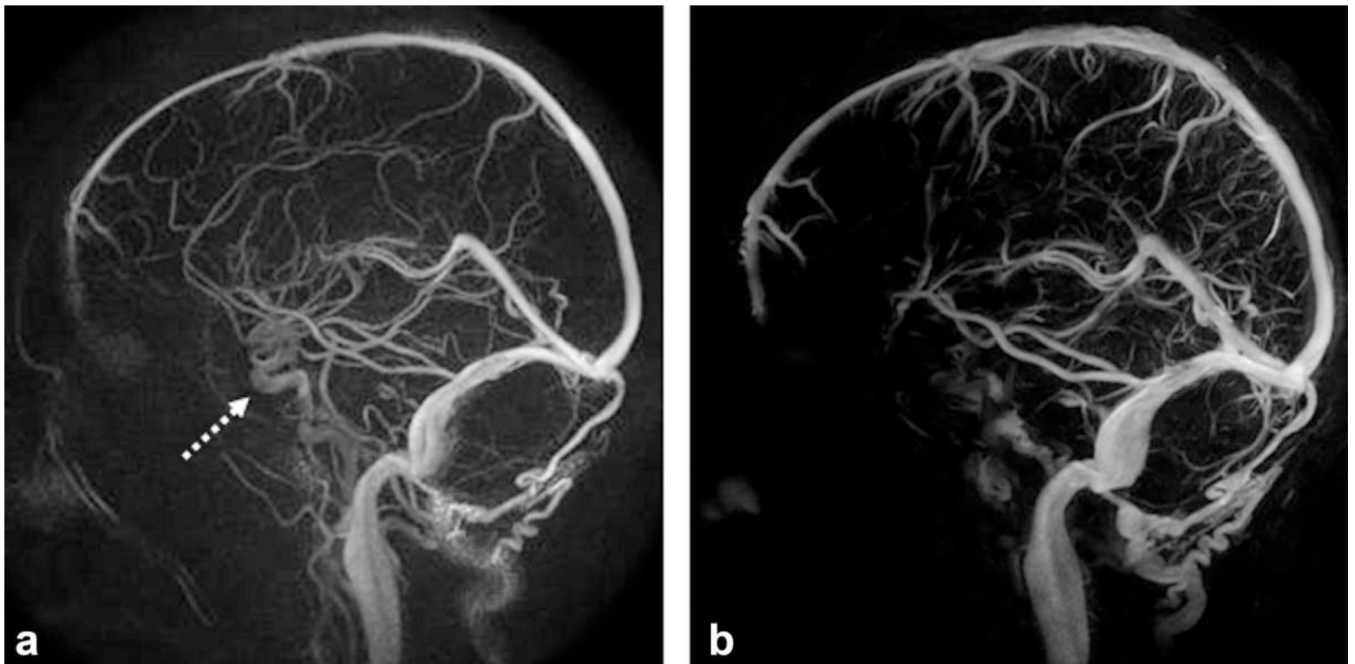


**FIG. 3.** Image comparison among low resolution VIPR reconstructed using gridding and zero-filling technique (a), HYPR CE (b), and high resolution CE image (c) from the same aneurysm patient. Line profiles across the aneurysm as shown in (c) were compared in (d). The aneurysm lumen from HYPR CE matches that from the high resolution CE image very well, where the VIPR shows significant blurring compared to the high resolution CE image.

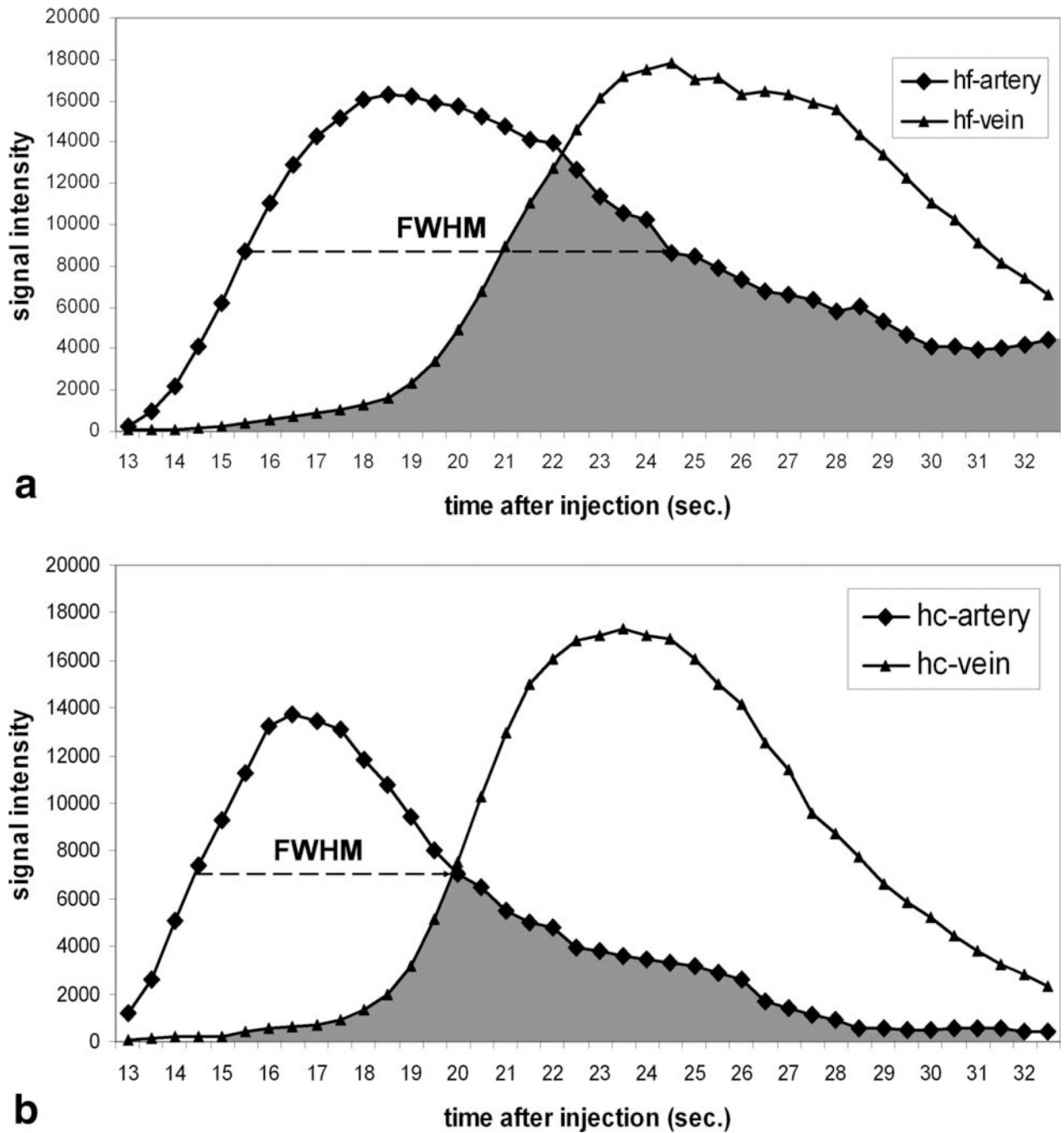


**FIG. 4.**

HYPR CE exam of a patient with dural Arteriovenous fistula. Arterial, mixed and venous phase images from the 60 frame HYPR CE exams are displayed in the axial, coronal and oblique views. Note the rapid enhancement of the left transverse sinus (arrows). On the oblique views a branch of the occipital artery supplying the dural arterio-venous fistula can be identified (arrowhead).



**FIG. 5.**  
**a:** The longer bolus length associated with the full dose injection for PC HYPRFLow results in partial overlap of the arterial and venous structures in this venous phase image (arrow). **b:** HYPR CE acquisition uses only 2 mL of contrast resulting in a shorter bolus and improved arterial to venous separation.

**FIG. 6.**

Example demonstrating the methods used to assess the arterial venous separation for (a) PC HYPRFlow and (b) HYPR CE. FWHM of the arterial curve from HYPR CE is significantly shorter than that from HYPRFlow. The overlap integral (shown as the shading area) from HYPR CE is significantly smaller than that from HYPRFlow.

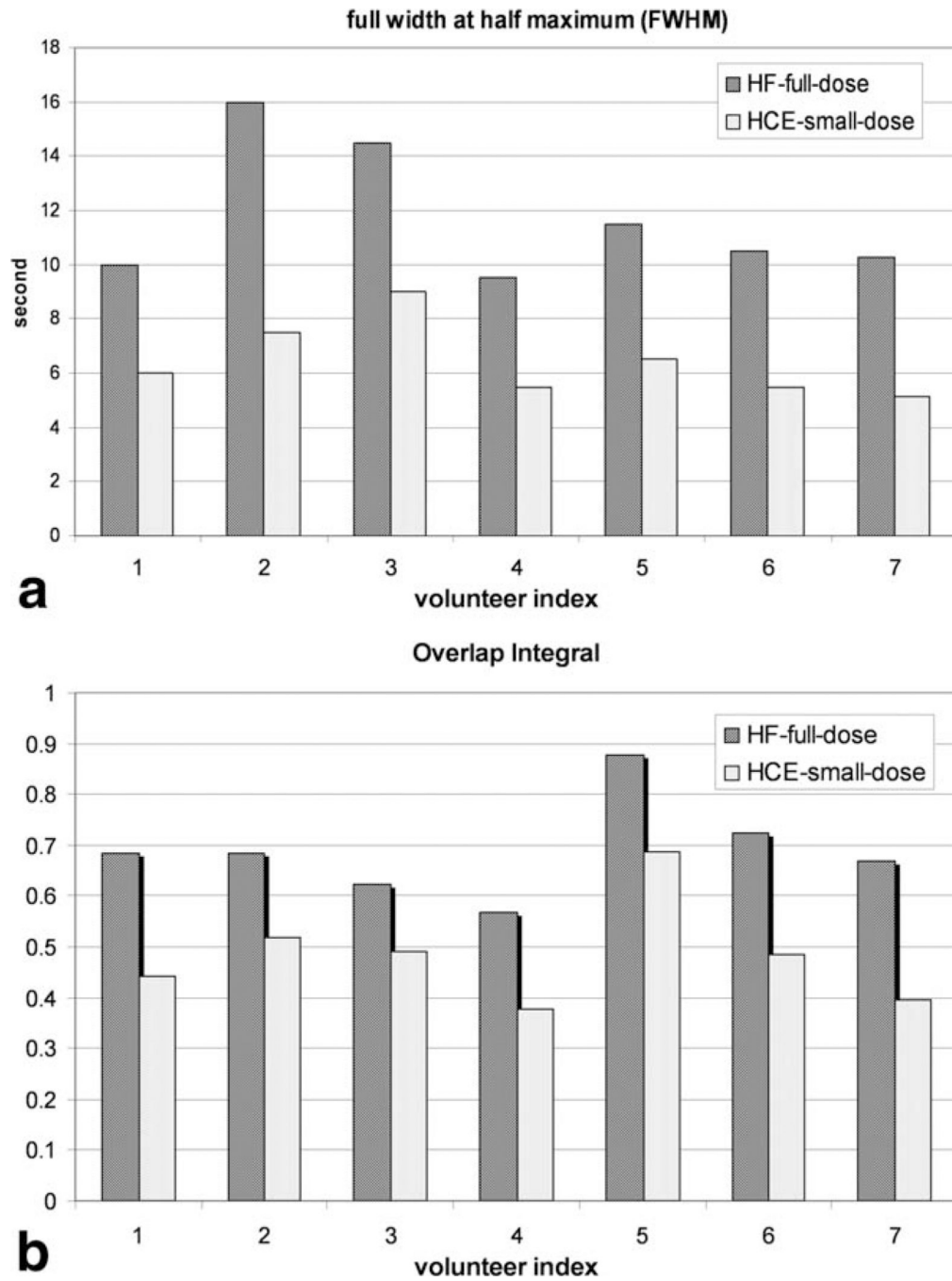


**FIG. 7.** Full width of half maximum (FWHM) (**a**) and overlap integral (**b**) calculated from HYPRFlow with full single dose (marked with HF-full-dose) and HYPR CE with single dose dual-injection techniques (HCE-small-dose) for seven volunteers.

**Table 1**

Mean  $\pm$  Standard Deviation of A/V Ratio, V/A Ratio, FWHM of Arterial Bolus (FWHM (A)), FWHM of Venous Bolus (FWHM (V)), and Overlap Integral (OI) for Volunteer Studies of Both HYPRFlow with Full Single Dose and HYPR CE with Single Dose Dual-Injection Techniques

	A/V ratio	V/A ratio	FWHM(A)	FWHM(V)	OI
HF-s*	3.56 $\pm$ 3.39	1.82 $\pm$ 0.29	11.8 $\pm$ 2.5	12.8 $\pm$ 2.5	0.689 $\pm$ 0.097
HCE-d*	20.36 $\pm$ 15.8	4.04 $\pm$ 1.4	6.4 $\pm$ 1.4	9.2 $\pm$ 2.0	0.485 $\pm$ 0.102
P-value*	0.023	0.0055	0.00009	0.0005	0.0000296

HF-s, HYPRFlow with full single dose injection; HCE-d, HYPR CE with single dose dual injection. P-value, based on two-tailed paired *t*-tests.